Solid amorphous formulations for enhancing solubility and inhibiting Erlotinib crystallization during gastric-to-intestinal transfer

Laura Mugnier, Fabienne Espitalier, Jérôme Menegotto, S. Bell, Maria-Inês Ré

Solid amorphous formulations for enhancing solubility and inhibiting Erlotinib crystallization during gastric-to-intestinal transfer

L. Mugnier[a], F. Espitalier[a], J. Menegotto[b], S. Bell[c] and M. I. Ré[a]

[a]Université de Toulouse, IMT Mines Albi, UMR CNRS 5302, Centre RAPSODEE, Albi, France; [b]EVOTEC, SAS, Toulouse, France; [c]Boehringer Ingelheim, Duluth, GA, USA

ABSTRACT

The objective of this study was to improve the solubility and inhibit the crystallisation during the gastric-to-intestinal transfer of Erlotinib (ERL), a small molecule kinase inhibitor (smKI) compound class, which is classified as class II drug in the Biopharmaceutical Classification System (BCS). A screening approach combining different parameters (solubility in aqueous media, inhibitory effect of drug crystallisation from supersaturated drug solutions) was applied to selected polymers for the development of solid amorphous dispersions of ERL. ERL solid amorphous dispersions formulations were then prepared with 3 different polymers (Soluplus®, HPMC-AS-L, HPMC-AS-H) at a fixed drug: polymer ratio (1:4) by two different production methods (spray drying and hot melt extrusion). The spray-dried particles and cryo-milled extrudates were characterized by thermal properties, shape and particle size, solubility and dissolution behavior in aqueous media. The influence of the manufacturing process on these solid characteristics was also identified during this study. Based on the obtained results, it is concluded that the cryo-milled extrudates of HPMC-AS-L displayed better performance (enhanced solubility, reduced ERL crystallization during the simulated gastric-to-intestinal transfer) and represents a promising amorphous solid dispersion formulation for oral administration of ERL.

KEYWORDS

Oral chemotherapy; solid amorphous dispersion; crystallization inhibition; solubility enhancement

Introduction

According to the World Health Organization (WHO), cancer remains one of the leading causes of death in the world. Approximately 70% of these deaths occur in low- and middle-income countries (WHO 2015). By 2050, the number of cancer patients is expected to double (Cabral and Kataoka 2014).

For the past 20 years, the pharmacological therapy of cancer has been undergoing a metamorphosis, rapidly changing from treatment with broad and unspecific cytotoxic agents to personalized and highly specific targeted agents. This therapy contains a new class of active pharmaceutical ingredients (APIs) which largely consists of small molecular compounds that mostly inhibit kinases (smKIs). Through their disruption of the kinase function, these targeted agents disrupt with multiple cancer signaling pathways which are essential to tumor development, survival, growth, and metastasis.

Alongside the advancing targeted therapy came the so-called 'intravenous-to-oral-switch' therapy. This is illustrated by an increasing number of marketed targeted oral anticancer APIs. Additionally, most of the targeted agents that are being investigated are intended to be administered orally.

Oral chemotherapy is a key step towards ''Chemotherapy at Home'', which is especially important for those cancer patients who are too weak to withstand harsh medical treatment. Oral chemotherapy is expected to maintain a sustained moderate plasma concentration of the API to achieve a prolonged exposure of cancerous cells to the API, as well as to avoid high Cmax (peak above the mean therapeutic concentration), resulting in much better efficacy and fewer side effects than the current intermittent parenteral chemotherapy.

A prerequisite for orally administered anticancer APIs (oncolytics) is a complete and predictable absorption process. For this, the API must be delivered from its pharmaceutical formulation in the gastrointestinal tract. The difficulty is that many oncolytic APIs are poorly soluble in water and consequently APIs are often inadequately absorbed, leading to incomplete and/or highly variable bioavailability. Moreover, many oncolytic APIs have a steep dose-response curve, and a dissolution-limited absorption increases the chance for a negative treatment outcome such as under-or over-dosing. In addition, numerous gastrointestinal side effects have been reported, such as diarrhea, cytotoxicity, dyspepsia, etc.

Because of the clear trends of oral oncolytics (Sawicki et al. 2016), it is expected that solubility-limited oral absorption will continue to challenge oral chemotherapy development. Poor aqueous solubility of an API entity can be addressed with various pharmaceutical particle technologies. Most of the commercially available oral oncolytics are physical mixture formulations, followed by prodrugs and lipid formulations. Non-conventional pharmaceutical formulations such as solid dispersions have been emerging, highlighting the feasibility and success of novel formulations, but they are still very scarce.

Erlotinib (ERL) belongs to the small molecule kinase inhibitor (smKI) compound class with the main feature being a pH-dependent solubility in water. Literature searches have revealed a diversity of experimental data on solubility of different forms of ERL at pH 1.2 and pH 6.8. At pH 6-7, the solubility of ERL, in the free base form, is between $3*10^{-6}$ and $7*10^{-6}$ g/g at 37 °C (Bhattacharya and Suryanarayanan 2009; Williams et al. 2018). The

low solubility at intestinal pH can lead to poor oral absorption, food-effects, and absorption related API – API interactions. Several formulation strategies have been applied to enhance ERL solubility and dissolution, including prodrugs, salt formation for weakly acidic or basic drugs, cocrystal, cyclodextrin complexation, emulsion/microemulsion/self-emulsifying systems, nano-drug delivery systems, and solid amorphous formulations (Kalepu and Nekkanti 2015; Han et al. 2019; Guan et al. 2021).

Solid amorphous formulations, in which the API exists in a solid amorphous state form with the assistance of carrier excipients, are regarded as one of the most promising techniques ascribed to rapid dissolution rate and superior absorption (Guan et al. 2021). Solid amorphous formulations of ERL were investigated using PVP (K25) (Jahangiri et al. 2022), PVP(K30) or PEG8000 (Huang and Gao 2009), HPMCS-M or HPMC E-3 (Miller and Morgen 2014), PL188 and Eudragit L100 (Meena and Choudhary 2019; Mudie et al. 2020) as carriers, however all published data have demonstrated the effect of ERL solubility enhancement in the gastric environment but not the inhibition of the ERL crystallization in the intestinal environment, which is one of the main obstacles for its oral administration.

In this study, ERL was formulated as solid amorphous dispersions aiming to increase the amount of soluble fraction at intestinal pH. The methodological approach applied is divided into several steps for screening of polymer candidates, production and characterization of solid amorphous formulations with selected polymers by two different production methods (spray drying and hot melt extrusion), both of which can move from the bench to an industrial scale and the investigation of the inhibitory effects of selected polymers on the dissolution kinetics of ERL from the corresponding amorphous solid formulations 2 h at gastric pH followed by 3 h at intestinal pH.

Materials and methods

Materials

Erlotinib Free base ((N-(3-ethynylphenyl)-6,7-bis(2-methoxyethoxy) quinazolin-4-amine); C22H23N3O4) was purchased from AMATEK (Purity 99%) and used as is. Acetonitrile and methanol (high-performance liquid chromatography grade) were purchased from VWR Chemicals. All other chemicals were of analytical reagent grade.

Five commercially available polymers were used for the study: Poly (ethylene glycol) grafted with a copolymer of poly (vinyl caprolactam) and poly(vinyl acetate) (Soluplus®, from BASF); Copolymer of poly(vinyl pyrrolidone) and poly(vinyl acetate) (Kollidon VA64, from BASF); Hypromellose Acetate Succinate with two different molecular weights 25800 Da and 21500 Da (HPMCAS-LG and HPMCAS-HG respectively, from Shin-Etsu Chemical AQOAT®); Hypromellose (HPMC 4 M, viscosity 4000 mPas, from Dupont). For an easier lecture, HPMCAS-LG and HPMCAS-HG will be called HPMC-L and HPMCAS-H respectively.

Screening of polymer candidates for ERL solid amorphous formulations

A screening of polymers has been done combining different parameters: calculation of solubility parameters, inhibitory effect of the polymer candidates on the crystallization of ERL from supersaturated solutions and ERL solubility in aqueous media in the presence of these polymers.

Solubility parameters

Solubility parameters (δ) have been used as a rapid screening tool for the selection of potential carrier polymers in solid dispersions, predicting if the API will dissolve in the carrier to form a solid solution (Greenhalgh et al. 1999; Jahangiri et al. 2022). The chemical structure of the compound ERL was drawn, and the solubility parameters determined by Van Krevelen and Hoftyzer's group contribution method by using the contributions for functional groups as reported in the literature using the following equation (Van Krevelen and Te Nijenhuis 2009):

$$\delta^2 = \delta_d^2 + \delta_p^2 + \delta_h^2 \quad (1)$$

Where, δ is the total solubility parameter, δ_d is contribution from dispersion forces, δ_p is contribution from polar forces, and δ_h is contribution from hydrogen bonding. For polymers, the solubility parameters (determined based on the single repeating monomer unit and the average molecular weight) were taken from the literature. The differences ($\Delta\delta$) between the solubility parameter values of the compound ERL and polymers were calculated.

Inhibitory effect of polymers on the crystallization of Erlotinib from supersaturated solutions

For amorphous solid dispersion, in addition to its stability in a given storage time, it is of great importance to prevent drug crystallization during dissolution in gastrointestinal tract. Crystal growth may occur leading to a reduction of soluble drug and compromising the solubility advantages. To avoid this problem, the crystal growth formation can be delayed or prevented by adding polymers as nucleation inhibitors (Greenhalgh et al. 1999; Jahangiri et al. 2022). Thus, various polymers were selected for screening the inhibitory effect on ERL crystallization from supersaturated aqueous-ethanolic solutions.

Firstly, ERL ($1*10^{-6}$ g/g) was dissolved in ethanol. An aliquot (5 ml) of the concentrated ERL ethanolic solution was then added to 50 ml of the aqueous medium (water or 10 mM pH 6.8 phosphate buffer), in which a weighed amount of polymer had been previously dissolved. A volume of 1.5 ml of the solution samples was taken out for ERL measurement by performance liquid chromatography (HPLC) at scheduled time intervals up to 120 - 180 min. The chromatographic system consisted of an Agilent system Infinity II 1290 (UHPLC) with a Kromaplus® C18 column used at ambient temperature (250 × 4.6 mm, 5 μm, ProtonSil). The mobile phase consisted of a mixture of Acetonitrile, 10 mM pH4 Ammonium Acetate Buffer and Methanol in the ratio 50:30:20 v/v respectively and a flow rate was set at 1.00 ml/min throughout the 10 min run. The 15 μL volume of sample was taken up by auto-sampler and was detected using UV detector at a wavelength of 254 nm. The column was maintained at 25 °C and retention time of ERL was about 7 min. Firstly, a standard solution was prepared with a concentration of $0.2*10^{-3}$ g/g of ERL in MeOH. Then, successive dilutions were performed in order to obtain the calibration curve. The concentrations were calculated with linear regression equation (Response (mAU) = 55 480 103 C (g/g solution) + 48.656; R2 = 0.9999) obtained with the linear ranges of calibration curve between peak area and the concentration (minimum value of $0.2.10^{-3}$ g/g solution). All concentrations are calculated using this calibration equation obtained in methanol. For the determination of the concentration in media different from methanol (water, biorelevant media, etc.), the calculated concentration was corrected by the density ratio of the two media. The density was measured with a glass pycnometer ($\rho_{methanol}/\rho_{medium}$). All measurements were performed in duplicate.

Effect of the polymer candidates on the aqueous solubility of Erlotinib

The equilibrium solubility of crystalline ERL in the test media (10 mM pH 6.8 phosphate buffer) was measured at 37 ± 0.5 °C in the presence and absence of the polymer candidates.

Accurately weighed polymer was added into flasks, which were pre-filled with 50 ml of phosphate buffer. Once the polymer completely visually dissolved, an excess ERL bulk powder was then put into each flask. The experimental procedure consisted of taking samples of the solution at various time points. Before any sampling, the stirring was stopped. The excess solid was allowed to settle for a few minutes. A sample of the supernatant taken with a syringe fitted with a needle was immediately centrifuged for 30 min at the same temperature as the experiment. The supernatant was then assayed by HPLC according to the method already described (section 2.2.2). All measurements were performed in duplicate. The solubility of pure ERL in absence of polymer has also been measured, using the same method.

ERL solid amorphous formulations

Preparation

After the polymer screening studies, both spray-drying and hot-melt extrusion processes were employed to prepare ERL solid amorphous formulations with 3 polymer candidates (Soluplus®, HPMCAS-H and HPMCAS-L) selected out of five from the screening phase.

Spray drying (SD) process. A Buchi B-290 mini-spray dryer (Buchi Labortechnik AG, Flawil, Switzerland) equipped with Inert Loop B-295 and an integrated two-fluid 0.7 mm nozzle was used for spray drying and all obtained powders were collected in glass containers and stored at room temperature in vacuum desiccators till further studies. The liquid formulations were prepared by dissolving ERL ($6 - 9*10^{-3}$ g/g) and the selected polymer ($20 - 22*10^{-3}$ g/g) in a 20:80 ethanol: distilled water mixture (w/w) to reach the desired ratio of ERL to polymer (1:4). The solutions were pumped at 31 ml/h and dried at 90-95 °C inlet and 50-55 °C outlet temperatures under an air-drying rate of 35 m^3/h (100% aspirator).

Hot-melt extrusion (HME) process. A mini-extruder HAAKE MiniLab 3 (Thermo scientific™, Germany) equipped with a co-rotating twin-screw parallel was used to generate the extruded samples. First, ERL and the selected polymer were accurately weighed and manually mixed to obtain physical mixtures. The physical mixtures were fed into the mini- extruder at 170 °C, a screw speed of 150 rpm with a residence time of 3 min. The hot melt extrudates were pushed through a die diameter of 1.5 mm, cooled, and cryo-grinded using the SPEX 6775 Cryogenic Mill (two cycles, total time of 9 min).

Solid state characterization

Thermal analyses. Thermal analyses were performed using a differential scanning calorimeter DSC Q200 with the base module and modulate-DSC (TA Instruments, USA). Samples were weighed (around 5 mg), placed in 100 μL pierced aluminium pans and then heated at a rate of 5 °C/min from 20 to 200 °C under a nitrogen flow of 50 ml/min. The analyses were made in non-hermetic aluminium pans, indium standards were used for enthalpy and temperature calibration and an empty aluminium pan was used as a blank. As for the modulation mode (mDSC), sapphire was used to calibrate in Cp. In mDSC, the heat rate was set up at 2 °C/min from 20 to 200 °C, with the modulation period of 40 s and amplitude 0.2 °C.

Scanning electron microscopy (SEM). SEM images were obtained using a scanning electron microscope Philips XL30 ESEM-FEG (Philips, USA) with acceleration voltage of 20 kV. Samples were fixed on a support using a double-sided adhesive and covered with platinum using a high-resolution SEM coated spray Polaron SC7640 (Quorom Technologies, England).

Particle size. Particle size measurements were performed with a laser diffractometer Mastersizer 3000 (Malvern Instruments, Malvern, UK) equipped with the dispersion module HYDRO MV (Malvern Panalytical). All measurements were performed in triplicate, by dispersing the powders in distilled water at ambient temperature. The particles were dispersed in water as the solid is very poorly soluble in water. Mie's theory was used to calculate the particle size distributions with the default refractive indices (Absorption Coefficient of 0.1 and Refractive Index of 1.52). Average particle size was expressed as the volume mean diameter [D4.3]. Polydispersity was given by Span index calculated by $(Dv_{90} - Dv_{10})/Dv_{50}$, where Dv_{90}, Dv_{50} and Dv_{10} are the particle diameters determined respectively at the 90th, 50th and 10th percentiles of undersized particles.

Supplementary analyses for selected samples. For a selected amorphous solid formulation demonstrating the best results in solubility and dissolutions studies, additional studies were performed to have some information concerning its physical stability.

Dynamic vapour sorption (DVS). An automated water sorption analyzer (DVS-2, Surface measurement systems Ltd., London, UK) was used. The relative humidity around the sample was controlled by mixing saturated and dry carrier gas streams using mass flow controllers. Prior to being exposed to any water vapor, the sample was dried at 0% RH to remove any water present. Next, the sample was exposed to the desired relative humidity and the moisture uptake was measured. For comparison purposes, pure ERL was also analyzed.

Stability monitoring study. A short stability study was also performed in accordance with the ICH guidelines at stability condition 25 °C/60% RH in closed glass containers. Samples of the selected amorphous solid formulation were monitored by DSC analysis immediately after production (T0), each 30 days, within 60 days.

Solubility and dissolution studies

Solubility measurements. The equilibrium concentration of ERL in distilled water at 37 ± 0.5 °C was measured from all solid formulations. Distilled water was filled into 50 ml-flasks and approximatively $0.1*10^{-3}$ g of each formulation was added into flasks separately. Then the experimental procedure was the same as described in section 2.2.3. All measurements were performed in duplicate.

Two-steps and pH change in vitro dissolution. Dissolution experiments were performed using a six-station dissolution rate test type II apparatus (ERWEKA DT 126 Light-DH1520, Germany), at 37 ± 0.5 °C with paddle speed at 75 rpm. Briefly, appropriate quantity of samples (containing 9 mg ERL in a capsule positioned in a sinker) was placed in 230 g of dissolution medium. Samples (1.5 ml) were collected at predetermined time intervals and

immediately centrifuged for 30 min at 150 × 100 rpm at 37 °C. The supernatant was collected and analyzed using HPLC method described above.

To be more representative of physiological conditions, the dissolution tests included two pH stages to mimic the gastrointestinal passage and were performed in biorelevant media. A Simulated Gastric Fluid (SGF), containing NaCl, Pepsin and HCl and a Fasted State Small Intestinal medium (FaSSIF), containing NaH_2PO_4, NaCl, Pepsin, Na taurocholate and Lecithin were used. Briefly, drug equivalent to $9*10^{-3}$ g of ERL was filled into the hard gelatine capsule (LGA, Incolore, Size 000) and performed in 200 ml of SGF medium at pH 1.2 for 2 h then 200 ml of FaSSIF medium were added in the dissolution vessel and the pH adjusted to 6.8 by NaOH addition. All experiments were conducted in triplicate. ERL concentration was determined by HPLC as previously described. ASD dissolution profiles were presented as concentration of the drug in solution vs. time. In all experiments, non-sink conditions were presented at pH 6.8 aiming to evaluate supersaturation performance. SI (Sink Index), defined as ***SI = Cs/(Dose/V)*** (Sun et al. 2016), where ***Cs*** is the solubility of crystalline API, V the volume of dissolution medium and Dose is the total amount of API in the test sample, was fixed at a constant value of 0.1 by adjusting the amount of ERL pure.

For comparison purposes, the dissolution profile of pure ERL was also evaluated in non-biorelevant media. Initially, the dissolution started with 230 ml of 0.1 M hydrochloric acid for 2 h. Subsequently, the pH was changed to 6.8 for additional 3 h with 70 ml of a mixture containing 0.4 M sodium phosphate buffer.

Results and discussions

Screening of polymers

Solubility parameters

Solubility parameters (δ) are widely used to identify miscible solvent-solute combinations in chemical and polymer applications. The rule of 'like dissolves like' applies, i.e. two materials with similar solubility parameters are expected to be miscible. In general, a combination of API and polymer with a difference in solubility parameter (Δδ) of 7.0 $MPa^{1/2}$ or less is considered miscible (Greenhalgh et al. 1999; Ghebremeskel et al. 2007; Van Krevelen and Te Nijenhuis 2009; Djuris et al. 2013; Sarode et al. 2013). The solubility parameters (δ) of ERL and five polymer candidates as well as the difference between the solubility parameter of ERL and each one of the polymers (Δδ) are given in Table 1. The conclusion of this first step of screening is the acceptance of the 5 polymers as they present an expected miscibility with ERL, with $\Delta\delta \leq 6$ $Mpa^{1/2}$. They were then selected for further evaluation.

Inhibitory effect of polymers on the crystallization of Erlotinib from supersaturated solutions

The inhibitory effect of polymers on the ERL crystallization from aqueous-ethanolic supersaturated solutions was tested at room temperature with water as aqueous medium. Figure 1 shows ERL concentrations reached between 2h and 3h in 1:10 ethanol:distilled water (w/w), in absence and presence of the five polymer candidates. The ranking order of polymer efficacy to maintain ERL in solution was HPMCAS-L > Soluplus®> HPMCAS-H > Kollidon VA64 > HPMC 4 M, with an increase in solubility of at least 1.3-fold compared to ERL alone.

From the results presented in Figure 1, the best polymers: HPMCAS-L, Soluplus®, HPMCAS-H, and Kollidon VA64 were chosen for further studies performed in 1:10 ethanol:phosphate buffer pH 6.8 at 37 °C. Figure 2 shows ERL concentrations reached between 2h and 3h in 1:10 ethanol: phosphate buffer pH 6.8 mixture, in absence and presence of the four tested polymers.

Comparing Figures 1 and 2, ERL concentrations reached in 1:10 ethanol:phosphate buffer pH 6.8 at 37 °C were lower than those in 1:10 ethanol:distilled water (w/w) at ambient temperature. The reason is the lower polymer concentration in the second series of experiments ($2.8*10^{-3}$ g/g) compared to the first one ($5*10^{-3}$ g/g). The effect of the polymer is proportional to its concentration. For example, for $2.8*10^{-3}$ g/g of HPMCAS-H in phosphate buffer (pH = 6.8) and 37 °C, ERL concentration is measured to be $20.6*10^{-6}$ g/g; while for $5.0*10^{-3}$g/g of HPMCAS-H in distilled water (pH = 6.3) and ambient temperature, ERL concentration was found to be $34*10^{6}$g/g.

Different mechanisms can be the reason of drug concentration enhancement, depending on the inhibitor in solution, such as reduction of molecular mobility of API molecules in solution, nucleation or crystal growth inhibition (Szafraniec-Szczęsny et al. 2021). Soluplus® is known to contribute to micellar solubilisation. Once the micelles are formed, Soluplus® can entrap drugs (Williams et al. 2013; Otsuka et al. 2015; Xia et al. 2016; Shi et al. 2017). Higher molecular weight polymers as HPMC 4 M might increase the local viscosity surrounding the dissolving drug delaying diffusion of the solubilized drug into bulk solution and then its crystallisation (Miller et al. 2008). HPMCAS has amphiphilic property as it consists of acetic acid and succinic acid esters of hydroxypropyl methyl cellulose. The L and H types of HPMCAS dissolve at pH 5.5 and 6.0 respectively, due to the different content of acetyl and succinyl groups of the polymer (Zhang et al. 2018). Polymers as HPMCAS has been found to be an effective inhibitor of drug crystal growth at both high and low levels of supersaturation, by adsorption of nuclei (Schram et al. 2015; Palmelund et al. 2016; Xie and Taylor 2016). However, inhibition of crystal growth does not mean inhibition of crystallization. Considering that ERL nanocrystals can be formed in presence of HPMCAS and to make sure to not take recrystallized ERL nanocrystals when measuring the concentration of ERL dissolved in the medium in presence of HPMCAS, the samples taken from the liquid medium were centrifuged before HPLC analysis.

Effect of polymer on ERL solubility in aqueous medium

Four polymers were selected from the previous inhibitory effect screening, HPMCAS-L, HPMCAS-H, Soluplus® and PVPVA64. Two of polymers chosen have a water solubility not dependent on pH (Soluplus®, PVAVA64) and two have a pH-dependent solubility in

Table 1. Estimated solubility parameter (δ) of compound ERL and polymer candidates.

Active Compound or Polymer	Solubility Parameter δ ($Mpa^{1/2}$)	Δδ (= δC - δP)[1] ($Mpa^{1/2}$)
ERLOTINIB (ERL)	23.1	–
HPMCAS-H or L	29.1 (Sarode et al. 2013)	6.0
Soluplus®	20.7 (Wlodarski et al. 2015)	2.4
Kollidon VA64	21.2 (Sarode et al. 2013)	1.9
HMPC 4 M	22.4 (Thiry et al. 2016)	0.7

[1]δC solubility parameter of compound ERL, δP solubility parameter of polymer, Δδ solubility parameter difference between compound ERL and polymer.

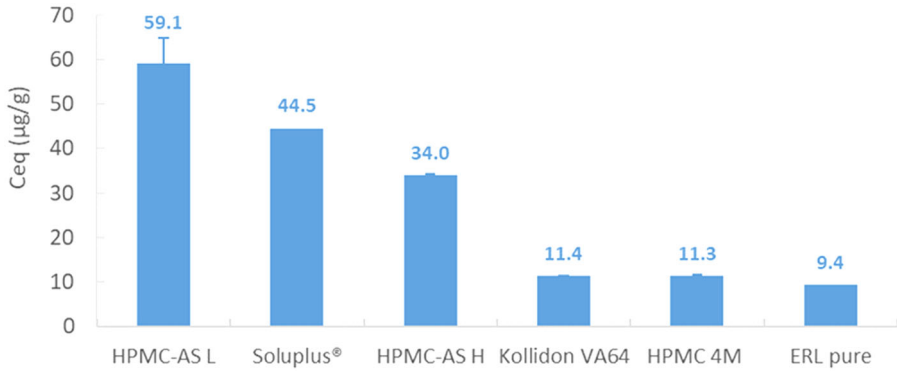

Figure 1. Erlotinib concentrations reached after 2-3h into 1:10 ethanol:water mixtures (w/w) with or without pre-dissolved polymers ($5*10^{-3}$ g/g), at ambient temperature.

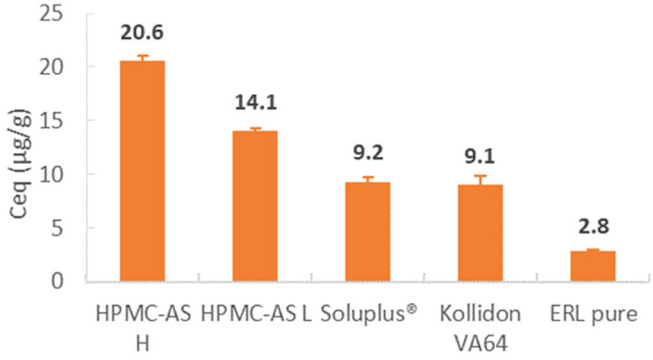

Figure 2. Erlotinib concentrations reached after 48h into 1:10 ethanol:phosphate buffer (w/w) pH 6.8 with or without pre-dissolved polymers ($2.8*10^{-3}$g/g), at 37 °C.

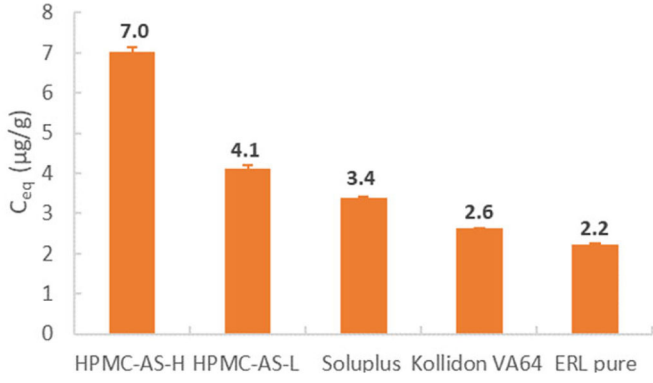

Figure 3. Solubility of Erlotinib in phosphate buffer pH6.8 at 37 °C, in presence or absence of pre-dissolved polymers ($0.5*10^{-3}$ g/g).

water (HPMCAS-L, HPMCAS-H). The polymer concentration was fixed at $0.5*10^{-3}$ g/g aiming to observe the effect of the polymer on ERL solubility in an aqueous medium under less favorable concentration condition than those fixed on the inhibitory effect studies.

Figure 3 shows the ERL equilibrium concentration in presence of each polymer and in absence of them. In presence of all studied polymers, ERL solubility enhanced from 1.2 to 3-fold times the solubility of ERL alone. The superiority of HPMCAS in increasing the ERL aqueous concentration is likely due to two properties. As already said before, HPMCAS is amphiphilic, and hydrophobic regions on the polymer provide sites for drug association, while hydrophilic regions permit the stable formation of hydrated nanosized colloidal structures in aqueous media. Second, above pH 5.0 the polymer is at least partially ionized, and this charge supports stable nanosized drug polymer aggregates (colloidal particles) which do not merge into larger aggregates which may not be capable of facile release of free drug. From these results, the two grades of HPMCAS (H and L) and Soluplus® were selected to verify the feasibility of producing ERL solid amorphous formulations, since they might provide different ERL supersaturating maintaining performance.

ERL solid amorphous formulations

The parameters studied were the type of polymer (HPMCAS-H, HPMCAS-L and Soluplus®) and the manufacturing process used. The ERL amorphous solid formulations were prepared using two different processes, spray drying and hot-melt-extrusion, both transferable to industrial scale, and this is the reason why they have been first tested in laboratory scale. The drug:polymer mass ratio was fixed at 1:4. The spray-dried particles and the cryo-milled extrudates produced were characterized (DSC analysis, SEM images, solubility, and dissolution studies).

Solid state characterization

DSC analyses. Figure 4 shows the DSC thermograms obtained for ERL formulations produced from SD and HME processes with Soluplus®, HPMCAS-H and HPMCAS-L (mass ratio 1:4). The figure also shows the DSC thermogram of physical mixtures between the unprocessed ERL crystals and Soluplus® in the same mass proportions of formulated powders, as well as for unprocessed ERL crystals alone. The thermal profile of unprocessed ERL crystals shows a distinct melting endotherm (Tm) at 155 °C with a melting enthalpy of 125.1 J/g/K. This value of Tm is close to that reported in the literature for the crystalline form of ERL free base (Williams et al. 2018). The physical mixture exhibits the same endotherm at 155 °C corresponding to the same ERL crystalline form. Contrarily, in the mDSC thermograms for spray-dried and hot-melt extruded mixtures of ERL-Soluplus® no melting peak was observed with the presence of a single glass transition temperature (obtained by the tangent method, the T_g value being determined at the inflection point as shown in Figure 4). The amorphous character of each solid ERL-Soluplus® formulation is confirmed. For powders formulated by spray drying and HME with HPMCAS (H and L grades), the amorphous state of ERL in processed samples was also confirmed.

Table 2 presents the T_g values determined from the first heating cycle in mDSC analyses for ERL and the 3 polymers used. The T_g value found for ERL is 42.7 °C. The polymer candidates have different T_g values (66.7 °C for Soluplus® and 120 °C for HPMCAS,

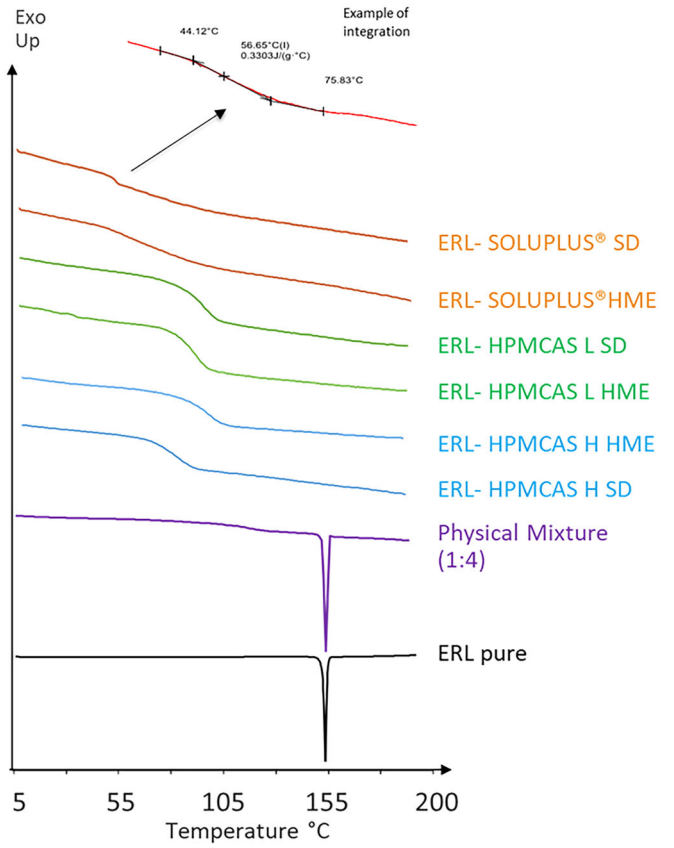

Figure 4. DSC for Erlotinib and physical mixtures (PM) and mDSC curves (1st heating cycle) for SD and HME powders formulated with Erlotinib and Soluplus ®; Erlotinib and HPMCAS-H; and Erlotinib and HPMCAS-L. DSC thermograms show-ing the heat flow total and mDSC thermograms showing the reverse heat flow on the y-axis.

Table 2. Experimental and theoretical T_g calculated by G-T equation for a mixture ERL: polymer in a mass proportion of 1:4.

Sample	T_g (°C)	ΔCp (J/g/K)	T_g Gordon-Taylor (°C)	ΔT_g
ERL	42.7	0.4472	-	-
SOLUPLUS®	66.7	0.1816	-	-
HPMCAS H and L	120.0	0.1811	-	-
ERL-SOLUPLUS® SD (1:4)	57.2	0.2984	57.6	0.4
ERL-SOLUPLUS® HME (1:4)	55.0	0.3114	57.6	2.6
ERL-HPMCAS H SD (1:4)	99.8	0.4318	92.7	7.1
ERL-HPMCAS H HME (1:4)	91.5	0.2202	92.7	1.2
ERL-HPMCAS L SD (1:4)	99.0	0.4585	90.5	8.5
ERL-HPMCAS L HME (1:4)*	94.7	0.4304	90.5	4.2

*post-milling.

both grades H and L). For these systems containing 20% ERL by mass, the solid forms exhibited amorphous features with only one intermediate glass transition within the temperature range between the two pure components, irrespective to the type of process technique used for manufacturing (SD or HME).

These experimental values of T_g were compared with theoretical values calculated from the Gordon-Taylor (G-T) equation (Baird and Taylor 2012):

$$T_g = \frac{w_1 Tg_1 + k w_2 Tg_2}{w_1 + k w_2} \quad (1)$$

where w_1 and w_2 are the weight fraction of each component, Tg_1 and Tg_2 are the glass transition temperature of each component, and the constant k in equation 2 is calculated from the corresponding heat capacity change of the pure components at their respective glass transition:

$$k = \frac{\triangle Cp_2}{\triangle Cp_1} \quad (2)$$

The heat capacity change (ΔCp_1) for pure amorphous ERL at the T_g is 0.4472 J/g/K, for Soluplus®, HPMCAS-L and HPMCAS-H (ΔCp_2) equal to 0.1816, 0.1811 and 0.2047 J/g/K, respectively.

Table 2 compares experimental and theoretical T_g calculated by G-T equation (Equation 2). The experimental T_g values of 20% ERL spray-dried and hot-melt-extruded particles (cryo-milled) are in reasonable agreement with the values calculated from the G-T equation (from 0.4 to 8.5 °C), with positive deviation in most cases, which indicates that one could expect some interactions between the active ingredient and the polymers, but this point would have to be studied further.

Shape and size. SEM images (Figure 5) give a general view of the morphology of ERL solid amorphous formulations. The type of polymer, Soluplus® or HPMCAS, influences on the T_g but also on the physical characteristics of the particles, while the grade of HPMCAS (H or L) does not appear to have any influence (the reason why only HPMCAS-L is presented). As shown in Figure 5a and c), the shape of the spray-dried particles was dependent on the polymer, the ERL solid amorphous particles containing Soluplus® (named ERL-Soluplus® SD), being more spherical and less agglomerated than those produced with HPMCAS-L (named ERL-HPMCAS-L SD).

SEM images in Figure 5 also display ERL solid amorphous particles produced from HME process and cryo-milled for particle size reduction. For a same composition (type of polymer and ERL concentration in the amorphous solid particles), SD and HME processes generated particles with different physical shapes, what can be seen by comparing Figures 5a and b) for Soluplus® and Figure 5c with 5d) for HPMCAS-L. The milled extrudates show irregular shaped, comparatively large granules with sharp breaking edges including some scratches corresponding to the milling process.

Particle size analyses were performed on the different solid samples and the characteristic diameters obtained from laser diffraction granulometry are presented in Table 3 in volume fractions. The particle size distribution is represented the particle diameters determined respectively at the 90th, 50th and 10th percentiles of undersized particles, the equivalent volume mean diameter D[4,3] and the particle size distribution width.

For spray-dried particles, the fine fraction, which corresponds to the Dv_{10} values, gives the smallest particle size of 2.9 µm for ERL-Soluplus®, while the largest fraction (Dv_{90}) gives 9.8 µm, revealing a narrow particle size distribution for this sample which is the smallest in size. The spray-dried particles formulated with HPMCAS are larger with a remarkable increase in size for Dv_{90}, which is reflected in Dv_{50}. By associating the particle size information to SEM images, the Dv_{90} increase is rather linked to a tendency to agglomeration of the spray-dried particles produced with HPMCAS grades. Comparing with the particle sizes for corresponding formulated particles produced by HME, the latter are at least 4-fold bigger than spray-dried particles, which could have an influence on the dissolution.

Particle size can decrease exponentially with time when milled (Suryanarayana 2001) but this also increases the chances of milling changing the physical and solid-state characteristics such as amorphous content of the HME formulation. The milling process of HME formulations was undertaken at cryogenic temperatures as previous studies have shown that, by milling at temperatures below the T_g, amorphous components of formulations retain their amorphous content (Descamps et al. 2007). No changes on T_g

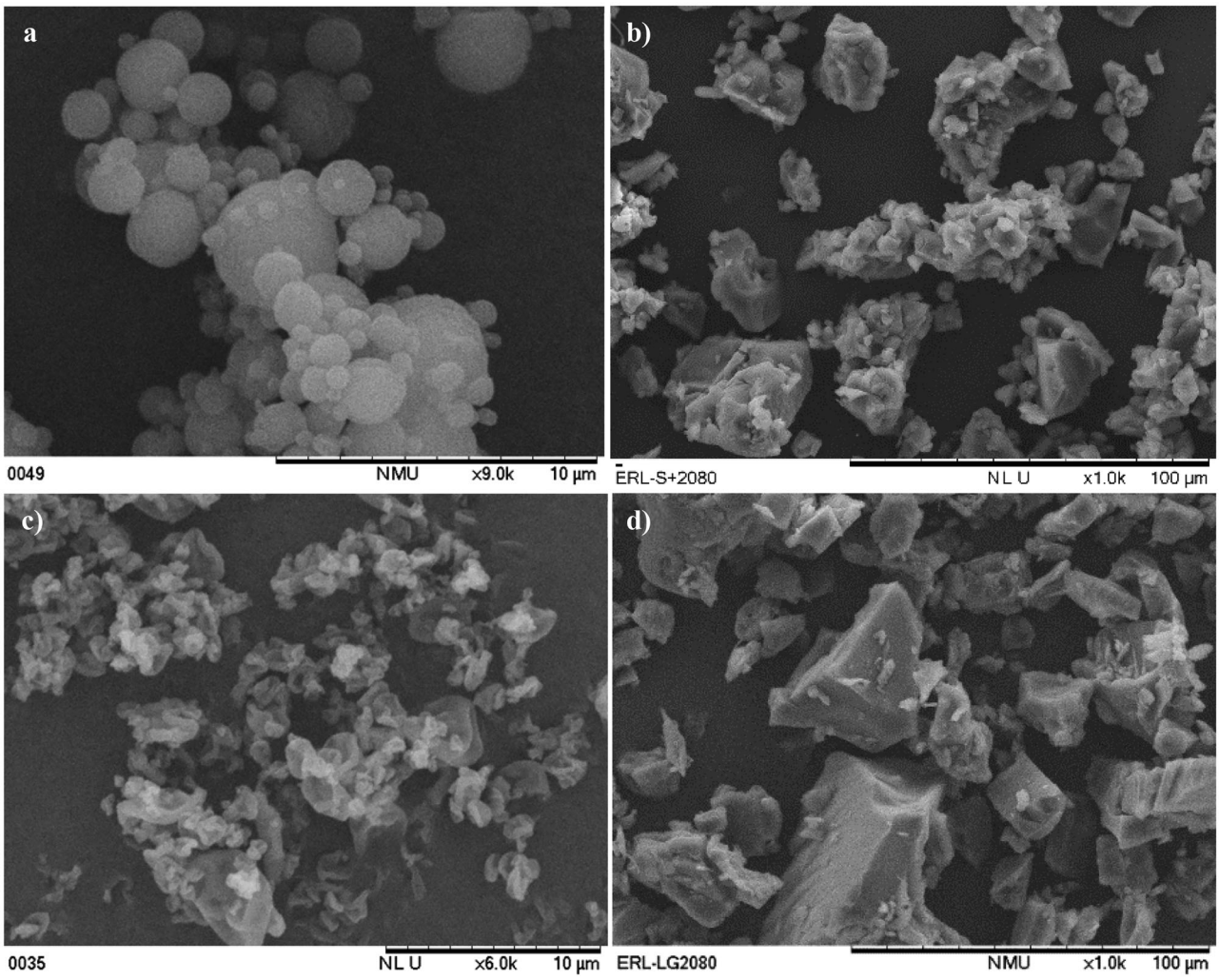

Figure 5. SEM images of amorphous solid particles a) Spray-dried ASD ERL-Soluplus® (ERL-Soluplus® SD); b) cryo-grinded extrudates ERL-Soluplus® (ERL-Soluplus ® HME); c) spray-dried ASD of ERL-HPMCAS-L (ERL-HPMCAS-L SD); d) cryo-grinded extrudates ERL-HPMCAS-L (ERL-HPMCAS-L HME).

Table 3. Particle size measurements from laser diffraction for all amorphous solid particles produced (ERL:Polymer 1:4).

	Characteristic diameters (µm)				
Sample	Dv_{10}	Dv_{50}	Dv_{90}	D[4,3]	Span
ERL	8.9	57.9	146.5	69.2	2.4
ERL-SOLUPLUS® SD	2.9	5.2	9.8	5.9	1.3
ERL-HPMCAS H SD	5.4	19.3	43.3	24.4	2.0
ERL-HPMCAS L SD	9.7	29.2	150.5	55.8	4.8
ERL-SOLUPLUS® HME*	5.4	27.6	58.8	30.4	1.9
ERL-HPMCAS H HME*	47.7	191.0	385.5	205.5	1.8
ERL-HPMCAS L HME*	27.7	83.4	228.0	107.5	2.4

*post-milling.

before and after cryo-milling was confirmed by DSC analyses (data not shown).

Solubility and dissolution studies

Solubility measurements. Measurements of ERL solubility from SD and HME solid formulations containing 20% ERL by mass have been performed in distilled water at 37 °C. As shown in Figure 6, it was found that the water solubility could be improved by formulation of ERL in an amorphous form with Soluplus® and with the two grades of HPMC-AS (L and H) and no crystallization was detected by a decrease in ERL concentration during the measurement. Results demonstrate that there seems to be an effect of the process on drug solubility, where HME better than SD particularly for ERL:HPMCAS formulations. Although it is well accepted that HME and SD are widely used to manufacture amorphous drug–polymer solid dispersions and are associated with ease of scale-up, the level of disorder of crystalline drug and homogeneity of drug distribution within the amorphous formulations can be different (Davis et al. 2018; Walsh et al. 2018), which could explain the different solubility results from spray-dried and cryo-milled extrudate particles shown in Figure 6.

Following those results, with the best solubility enhancement with the polymer HPMCAS from both processes, it has been chosen for further studies. Thus, ERL dissolution experiments were performed on ERL solid amorphous formulations obtained with both grades of HPMCAS.

Dissolution studies. Dissolution experiments were performed to evaluate the release rate profile from the solid amorphous formulations containing 20% ERL by mass at pH 1.2, followed by pH 6.8. Non-sink conditions (SI = 0.1) were applied, and all experiments were performed with a fixed maximum ERL concentration (approximately $9*10^{-3}$ g). Figure 7 displays the dissolution curves for pure ERL at pH 1.2 followed by pH 6.8 in buffer solution (orange curve), and in biorelevant media (blue curve). For pure ERL at pH 1.2, results were given up to 60 min and to 90 min at

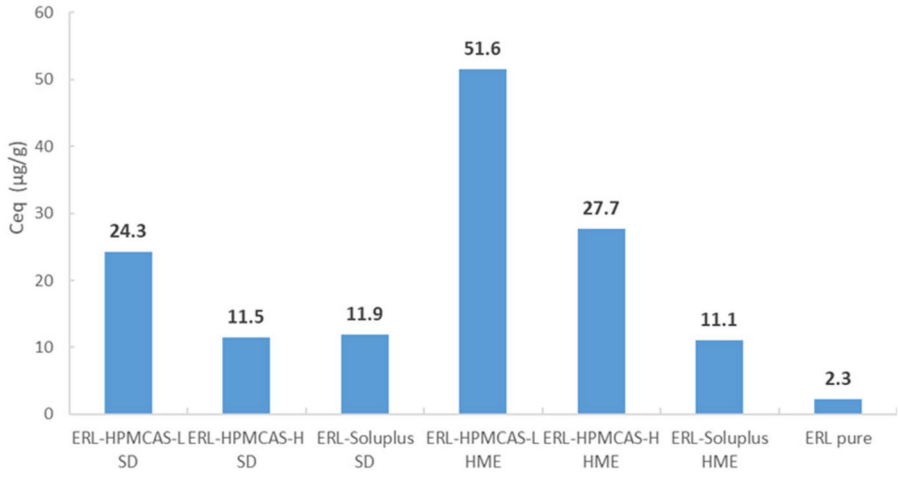

Figure 6. Solubility of Erlotinib in distilled water at 37 °C from amorphous solid formulations containing 20%ERL by mass and produced with soluplus®, HPMCAS (two grades) by SD and HME processes.

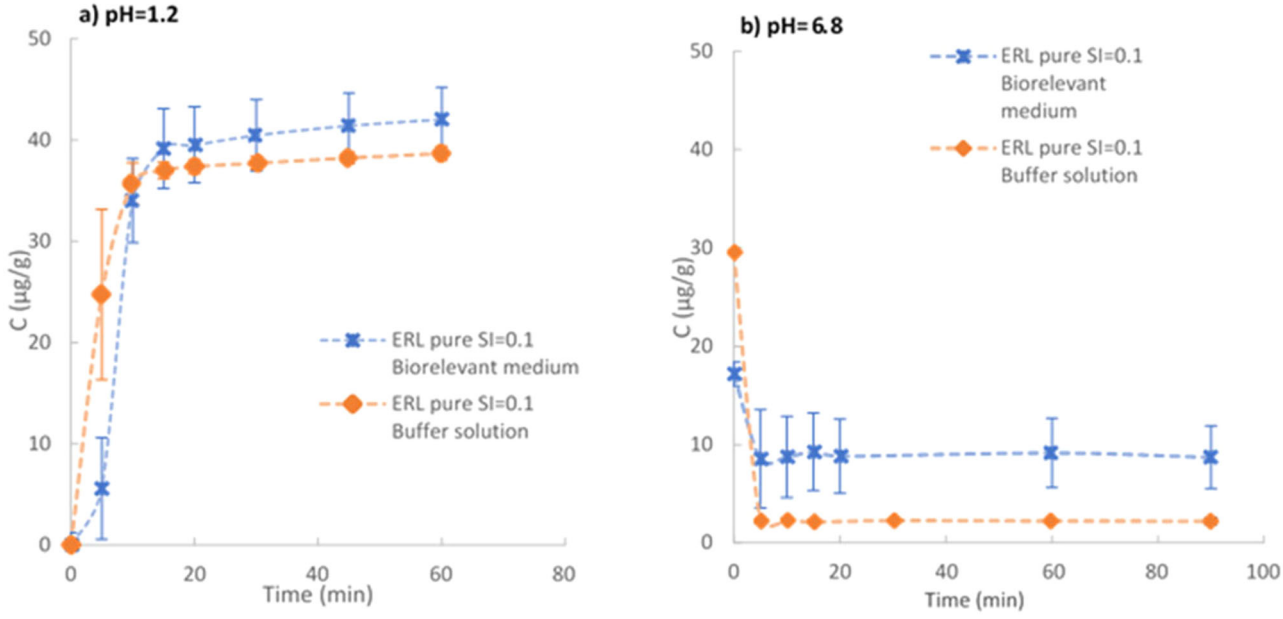

Figure 7. Dissolution profiles of raw ERL crystals at 37°C in different media: buffer solutions and biorelevant media: pH1.2 (a) and pH6.8 (b), SI=0.1.

pH 6.8. The theoretical concentration of ERL that could have reached if all the ERL dissolved (C_{max} ERL) at pH 1.2 and pH 6.8 are $39.9*10^{-6}$ and $30*10^{-6}$ g/g respectively. As it can be seen in Figure 7a, the dissolution of ERL at pH1.2 is total reaching C_{max} ERL in the medium after about 20 min; with the change of pH from pH1.2 to pH6.8 the ERL concentration drops drastically, as shown in Figure 7b. The presence of a plateau at about 10 min gives the value of the saturation concentration of the ERL in the dissolution medium at pH6.8. It is noticeable that ERL concentration is 4-fold higher at pH6.8 in biorelevant medium than in buffer solution. In addition to a stable phosphate buffer system, biorelevant medium contains bile salts and phospholipids (lecithin). These compounds facilitate the wetting of solids and the solubilization of lipophilic drugs into mixed micelles. This is the reason why dissolution of ERL may be enhanced considerably over the rate observed in simple aqueous solutions. The biorelevant environment was chosen for the dissolution studies of the ERL amorphous formulations with HPMCAS.

For the solid amorphous formulations obtained with HPMCAS-H and HPMCAS-L, ERL release was followed given up to 120 min at pH 1.2 and about 165 min at pH 6.8 and the results are shown in Figure 8. At pH 1.2 (Figure 8a), the maximum ERL concentration reached after 90 min was close to C_{max} ERL ($39*10^{-6}$ g/g), however, the dissolution profiles show that rates of dissolution and cumulative amounts were less for melt-extruded batches compared with corresponding spray-dried formulations.

Cryo-milled extrudates are about 4-fold bigger than spray-dried products, with less hydrophilic surface area. The formulation is also subjected to high intensity mixing and pressure during HME that lead to the free space present in the polymeric matrix to be reduced resulting in a low porosity polymeric matrix (Mahmah et al. 2014), dissolving slowly. For an absolute comparison an identical particle size would be best, although this would require a very small sieve fraction from the milled extrudate (or use of a jet mill) and a further enhancement of spray dried particle size. This could be achieved using alternative spray drying parameters, such as a pressure nozzle (Beyerinck et al. 2010). However, as already mentioned, besides particle size the level of interaction between drug and polymer which can be affected by the manufacturing process is also another process effect not to be underestimated.

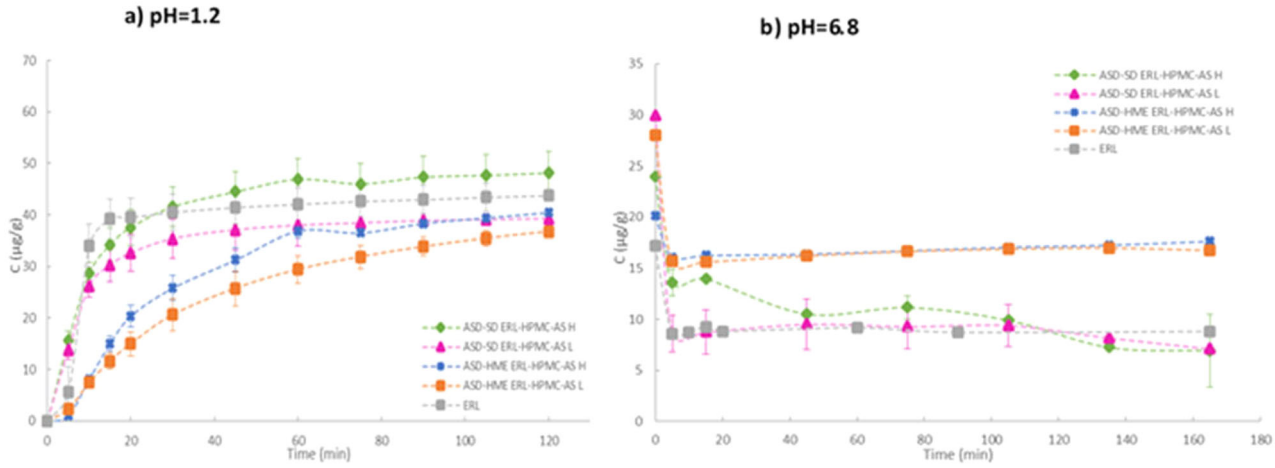

Figure 8. Dissolution kinetics of the Erlotinib solid dispersion (1:4) at 37 °C in different dissolution media: a) pH 1.2 (SGF medium); b) at pH 6.8 (FaSSIF medium), where 'SD': spray-dried and 'HME': Hot-Melt extruded + cryo-grinded, SI = 0.1.

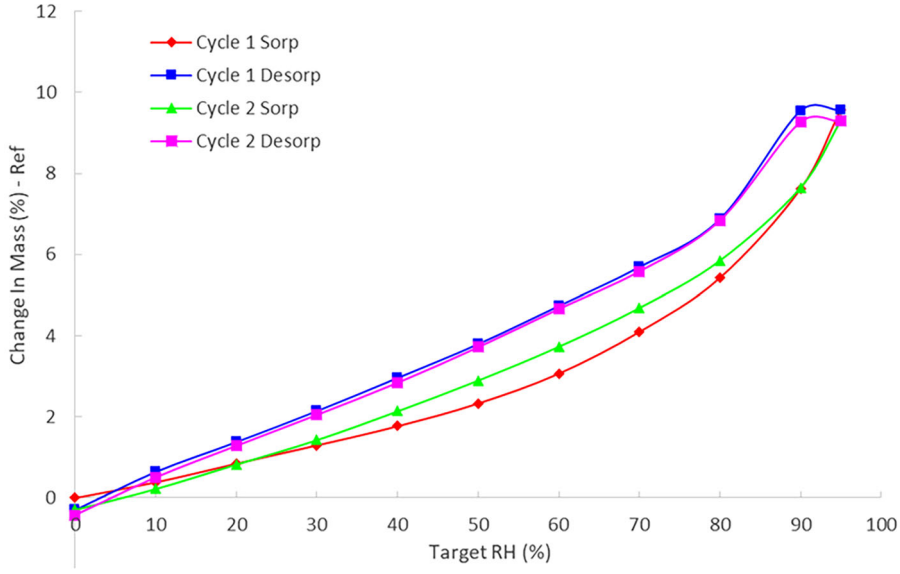

Figure 9. Moisture absorption profile of HME ERL-HPMCAS L formulation at 25 °C.

Table 4. Tg obtained from the stability study for the formulation ERL-HPMCAS L at 25 °C/60% RH.

	T (°C) ΔCp (J/g/K)		
Sample in open vial	T0	T1month	T2months
ERL-HPMCAS L HME	94.69 0.4304	97.85 0.4016	98.25 0.3644

However, it is well-known that the small intestine is the major site for drug absorption and where recrystallization must be avoided. As shown in Figure 8b), the concentration of ERL almost 2-fold higher than pure ERL was found with the two formulations (ERL:HPMCAS) produced by HME as manufacturing process.

The superiority of HPMCAS to maintain higher ERL concentration at pH 6.8 as already discussed can be due to the amphiphilic nature of this polymer with hydrophobic regions providing sites for drug association and hydrophilic regions keeping stable hydrated nanosized colloidal structures formed in the aqueous medium. Due to the pH-dependent solubility of HPMCAS, it is important to note that the polymer is not completely dissolved in the first minutes after adjustment of pH at 6.8. It dissolves slowly which creates a competition between the polymer in solution and the molecule in solution, so the effect of the polymer is diminished.

However, from the obtained results the influence of the manufacturing process is evidenced. It could be linked to the level of disorder of the solid state of the drug and homogeneity of drug distribution within the amorphous formulations. Although it is well accepted that HME and SD are widely used to manufacture amorphous drug–polymer solid dispersions and are associated with ease of scale-up, the level of disorder of the solid state of the drug and homogeneity of drug distribution within the amorphous formulations can be different (Davis et al. 2018; Walsh et al. 2018), which, besides differences on particle sizes, could explain different solubility results from spray-dried and cryo-milled extrudate particles shown in Figure 6.

Considering ERL-HPMCAS L HME a choice formulation as it demonstrated the best results in solubility and dissolutions studies, supplementary analyses were performed on this formulation aiming to have some information concerning its physical stability. On one side, a water sorption isotherm at 25 °C was used to obtain information about the affinity between the chosen

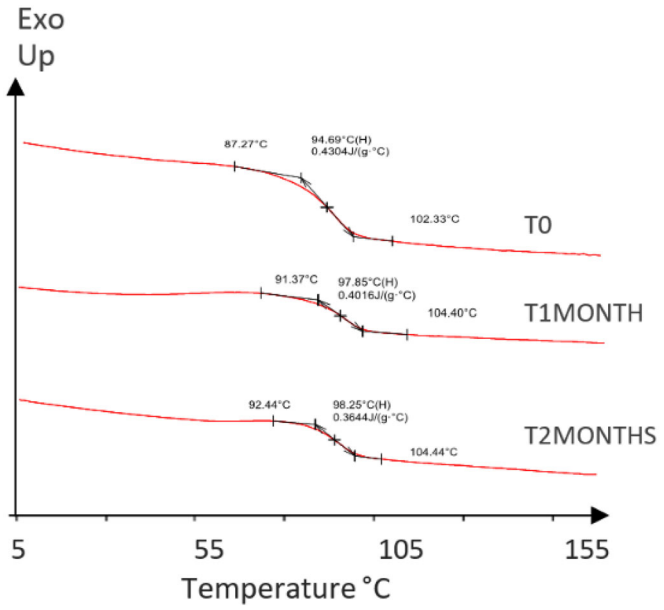

Figure 10. mDSC curves (1st heating cycle) for ERL-HPMCAS L formulation dur-ing the stability study in Open vials exposed at 25 °C/60% RH: T0; T1 month and T2 months.

formulation and water, upon exposure to stressed humidity. Figure 9 displays the DVS isotherm plots for the studied sample, showing the change in mass percentage as a function of changing relative humidity (RH) in the range 0 to 95% RH. The measured sorption over the RH 0-95% is a contribution of both adsorption (surface phenomenon) and absorption (volume phenomenon). Water vapor is absorbed into structure of amorphous solids and not simply adsorbed on the surface.

Firstly, the hydrophobic character of pure ERL was demonstrated by the water intake, which was very weak, the signal was in the noise of the scale. The ERL-HPMCAS L HME formulation was more sensitive to environmental moisture than the pure ERL, as shown by its measured water sorption isotherm (9.5% water content at equilibrium at 95% RH, Figure 9).

As water absorbed can act as a plasticizer and increase molecular mobility due to the breakage of hydrogen bonds between molecules (Repka and McGinity 2000), a 2-months stability study was also performed on ERL-HPMCAS L solid formulation, in accordance with the ICH guidelines at stability condition 25 °C/60% RH. The mDSC curves and Tg results are respectively shown in Figure 10 and in Table 4. It is noticeable that the samples have not evolved over time during the studied period since T_g of the mixture remains constant, which is a preliminary indication of physical stability in time. However, it must be confirmed by a longer stability study performed with solid state monitoring or a shorter stability study under harsher conditions (40 °C/75% RH).

Conclusion

In the present study, a screening approach has been conducted for the choice of 3 polymers (Soluplus®, HPMC-AS-L, HPMC-AS-L) that would improve the solubility and the inhibition of crystallization of ERL in biorelevant medium and during the gastric-to-intestinal route. Every three polymers led to amorphous solid formulations of ERL at a mass ratio of 1:4 manufactured by spray drying and hot-melt-extrusion processes followed by cryo-milling for extrudates particle reduction. Cryo-milled extrudates are approximately 4 times larger than spray-dried powders. The effect of manufacturing process was evidenced, being better for HME. Although the effect on dissolution kinetics must be partly due to physical differences that could not be minimized between SD and HME solid particles, the effect of the manufacturing process on solubility enhancement and ERL crystallisation inhibition in the simulated gastric-to intestine transfer is probably related to the level of intimate mixing between ERL and polymer which may have been favoured with HME. Finally, from the results obtained, an amorphous ERL solid formulation which could be promising for improving ERL oral bioavailability was identified.

Acknowledgements

The authors are grateful to P. Accart, S. Del Confetto, V. Nallet, S. Patry and C. Rolland from RAPSODEE Center for respectively analyses of particle size, DSC, XRD, DVS and SEM.

Disclosure statement

No potential conflict of interest was reported by the authors.

Funding

Research reported in this publication was supported by Boehringer Ingelheim Animal Health.

References

Baird JA, Taylor LS. 2012. Evaluation of amorphous solid dispersion properties using thermal analysis techniques. Adv Drug Deliv Rev. 64(5):396–421. doi:10.1016/j.addr.2011.07.009. Beyerinck RA, Ray RJ, Dobry DE, Settell DM. 2010. Method for making homogeneous spray-dried solid amorphous drug dispersions using pressure nozzles (United States Patent No. US7780988B2).

Bhattacharya S, Suryanarayanan R. 2009. Local mobility in amorphous pharmaceuticals—characterization and implications on stability. J Pharm Sci. 98(9):2935–2953. doi:10.1002/jps.21728.

Cabral H, Kataoka K. 2014. Progress of drug-loaded polymeric micelles into clinical studies. J Control Release. 190:465–476. doi:10.1016/j.jconrel.2014.06.042.

Davis MT, Potter CB, Walker GM. 2018. Downstream processing of a ternary amorphous solid dispersion: the impacts of spray drying and hot melt extrusion on powder flow, compression and dissolution. Int J Pharm. 544(1):242–253. doi:10.1016/j.ijpharm.2018.04.038.

Descamps M, Willart JF, Dudognon E, Caron V. 2007. Transformation of pharmaceutical compounds upon milling and comilling: the role of Tg. J Pharm Sci. 96(5):1398–1407. doi:10.1002/jps.20939.

Djuris J, Nikolakakis I, Ibric S, Djuric Z, Kachrimanis K. 2013. Preparation of carbamazepine–Soluplus® solid dispersions by hot-melt extrusion, and prediction of drug–polymer miscibility by thermodynamic model fitting. Eur J Pharm Biopharm. 84(1):228–237. doi:10.1016/j.ejpb.2012.12.018.

Ghebremeskel AN, Vemavarapu C, Lodaya M. 2007. Use of surfactants as plasticizers in preparing solid dispersions of poorly soluble API: selection of polymer–surfactant combinations using solubility parameters and testing the processability. Int J Pharm. 328(2):119–129. doi:10.1016/j.ijpharm.2006.08.010.

Greenhalgh DJ, Williams AC, Timmins P, York P. 1999. Solubility parameters as predictors of miscibility in solid dispersions. J Pharm Sci. 88(11):1182–1190. doi:10.1021/js9900856.

Guan Q, Ma Q, Zhao Y, Jiang X, Zhang H, Liu M, Wang Z, Han J. 2021. Cellulose derivatives as effective recrystallization inhibitor for ternary ritonavir solid dispersions: in vitro-in vivo evaluation. Carbohydr Polym. 273:118562. doi:10.1016/j.carbpol.2021.118562.

Han R, Xiong H, Ye Z, Yang Y, Huang T, Jing Q, Lu J, Pan H, Ren F, Ouyang D. 2019. Predicting physical stability of solid dispersions by machine learning techniques. J Control Release. 311–312:16–25. doi:10.1016/j.jconrel.2019.08.030.

Huang L, Gao S. 2009. Hydrochloride and its solid amorphous dispersion.

Jahangiri A, Khalilzad F, Barghi L. 2022. Dissolution improvement of binary solid dispersions of erlotinib prepared by one-step electrospray method. Biol Methods Protoc. 7(1):bpac001. doi:10.1093/biomethods/bpac001.

Kalepu S, Nekkanti V. 2015. Insoluble drug delivery strategies: review of recent advances and business prospects. Acta Pharm Sin B. 5(5):442–453. doi:10.1016/j.apsb.2015.07.003.

Mahmah O, Tabbakh R, Kelly A, Paradkar A. 2014. A comparative study of the effect of spray drying and hot-melt extrusion on the properties of amorphous solid dispersions containing felodipine. J Pharm Pharmacol. 66(2):275–284. doi:10.1111/jphp.12099.

Meena K, Choudhary D. 2019. Enhancement of solubility and dissolution rate of erlotinib hydrochloride by solid dispersion technique with poloxamer 188: preparation and in-vitro evaluation.

Miller DA, DiNunzio JC, Yang W, McGinity JW, Williams RO. 2008. Enhanced in vivo absorption of itraconazole via stabilization of supersaturation following acidic-to-neutral pH transition. Drug Dev Ind Pharm. 34(8):890–902. doi:10.1080/03639040801929273.

Miller WK, Morgen MM. 2014. Solid dispersions of low-water solubility actives (World Intellectual Property Organization Patent No. WO2014126969A1). https://patents.google.com/patent/WO2014126969A1/en?oq=2014/126969.

Mudie DM, Buchanan S, Stewart AM, Smith A, Shepard KB, Biswas N, Marshall D, Ekdahl A, Pluntze A, Craig CD, et al. 2020. A novel architecture for achieving high drug loading in amorphous spray dried dispersion tablets. Int J Pharm X. 2:100042. doi:10.1016/j.ijpx.2020.100042.

Otsuka N, Ueda K, Ohyagi N, Shimizu K, Katakawa K, Kumamoto T, Higashi K, Yamamoto K, Moribe K. 2015. An insight into different stabilization mechanisms of phenytoin derivatives supersaturation by HPMC and PVP. J Pharm Sci. 104(8):2574–2582. doi:10.1002/jps.24527.

Palmelund H, Madsen CM, Plum J, Müllertz A, Rades T. 2016. Studying the propensity of compounds to supersaturate: a practical and broadly applicable approach. J Pharm Sci. 105(10):3021–3029. doi:10.1016/j.xphs.2016.06.016.

Repka MA, McGinity JW. 2000. Influence of vitamin E TPGS on the properties of hydrophilic films produced by hot-melt extrusion. Int J Pharm. 202(1–2):63–70. doi:10.1016/S0378-5173(00)00418-X.

Sarode AL, Sandhu H, Shah N, Malick W, Zia H. 2013. Hot melt extrusion (HME) for amorphous solid dispersions: predictive tools for processing and impact of drug–polymer interactions on supersaturation. Eur J Pharm Sci. 48(3):371–384. doi:10.1016/j.ejps.2012.12.012.

Sawicki E, Schellens JHM, Beijnen JH, Nuijen B. 2016. Inventory of oral anticancer agents: pharmaceutical formulation aspects with focus on the solid dispersion technique. Cancer Treat Rev. 50:247–263. doi:10.1016/j.ctrv.2016.09.012.

Schram CJ, Taylor LS, Beaudoin SP. 2015. Influence of polymers on the crystal growth rate of felodipine: correlating adsorbed polymer surface coverage to solution crystal growth inhibition. Langmuir. 31(41):11279–11287. doi:10.1021/acs.langmuir.5b02486.

Shi N-Q, Zhang Y, Li Y, Lai H-W, Xiao X, Feng B, Qi X-R. 2017. Self-micellizing solid dispersions enhance the properties and therapeutic potential of fenofibrate: advantages, profiles and mechanisms. Int J Pharm. 528(1–2):563–577. doi:10.1016/j.ijpharm.2017.06.017.

Sun DD, Wen H, Taylor LS. 2016. Non-sink dissolution conditions for predicting product quality and in vivo performance of supersaturating drug delivery systems. J Pharm Sci. 105(9):2477–2488. doi:10.1016/j.xphs.2016.03.024.

Suryanarayana C. 2001. Mechanical alloying and milling. Prog Mater Sci. 46(1):1–184. doi:10.1016/S0079-6425(99)00010-9.

Szafraniec-Szczęsny J, Antosik-Rogóż A, Kurek M, Gawlak K, Górska A, Peralta S, Knapik-Kowalczuk J, Kramarczyk D, Paluch M, Jachowicz R. 2021. How does the addition of Kollidon®VA64 inhibit the recrystallization and improve ezetimibe dissolution from amorphous solid dispersions? Pharmaceutics. 13(2):147. doi:10.3390/pharmaceutics13020147.

Thiry J, Lebrun P, Vinassa C, Adam M, Netchacovitch L, Ziemons E, Hubert P, Krier F, Evrard B. 2016. Continuous production of itraconazolebased solid dispersions by hot melt extrusion: Preformulation, optimization and design space determination. International Journal of Pharmaceutics. 515(1): 114–124. doi: 10.1016/j.ijpharm.2016.10.003.

Van Krevelen DW, Te Nijenhuis K. 2009. Properties of polymers: their correlation with chemical structure; their numerical estimation and prediction from additive group contributions. Chapter 7 - Cohesive Properties and Solubility, Pages 189-227, ISBN 978-0-08-054819-7 (Fourth edition) Elsevier.

Walsh D, Serrano DR, Worku ZA, Madi AM, O'Connell P, Twamley B, Healy AM. 2018. Engineering of pharmaceutical cocrystals in an excipient matrix: spray drying versus hot melt extrusion. Int J Pharm. 551(1-2):241–256. doi:10.1016/j.ijpharm.2018.09.029.

Williams HD, Ford L, Han S, Tangso KJ, Lim S, Shackleford DM, Vodak DT, Benameur H, Pouton CW, Scammells PJ, et al. 2018. Enhancing the oral absorption of kinase inhibitors using lipophilic salts and lipid-based formulations. Mol Pharm. 15(12):5678–5696. doi:10.1021/acs.molpharmaceut.8b00858.

Williams HD, Trevaskis NL, Charman SA, Shanker RM, Charman WN, Pouton CW, Porter, CJ, H. 2013. Strategies to address low drug solubility in discovery and development. Pharmacol Rev. 65(1):315–499. doi:10.1124/pr.112.005660.

Wlodarski K, Sawicki W, Haber K, Knapik J, Wojnarowska Z, Paluch M, Lepek P, Hawelek L, Tajber L. 2015. Physicochemical properties of tadalafil solid dispersions – Impact of polymer on the apparent solubility and dissolution rate of tadalafil. Eur J Pharm Biopharm. 94:106–115. doi:10.1016/j.ejpb.2015.04.031.

World Health Organization. 2015 Feb 3. Cancer. https://www.who.int/en/news-room/fact-sheets/detail/cancer.

Xia D, Yu H, Tao J, Zeng J, Zhu Q, Zhu C, Gan Y. 2016. Supersaturated polymeric micelles for oral cyclosporine A delivery: the role of Soluplus–sodium dodecyl sulfate complex. Colloids Surf B Biointerfaces. 141:301–310. doi:10.1016/j.colsurfb.2016.01.047.

Xie T, Taylor LS. 2016. Improved release of celecoxib from high drug loading amorphous solid dispersions formulated with polyacrylic acid and cellulose derivatives. Mol Pharm. 13(3):873–884. doi:10.1021/acs.molpharmaceut.5b00798.

Zhang Q, Zhao Y, Zhao Y, Ding Z, Fan Z, Zhang H, Liu M, Wang Z, Han J. 2018. Effect of HPMCAS on recrystallization inhibition of nimodipine solid dispersions prepared by hot-melt extrusion and dissolution enhancement of nimodipine tablets. Colloids Surf B Biointerfaces. 172:118–126. doi:10.1016/j.colsurfb.2018.08.030.